Available online at www.sciencedirect.com
SCIENCE DIRECT®

Journal of the European Ceramic Society 23 (2003) 1803–1811
www.elsevier.com/locate/jeurceramsoc

Hydroxyapatite formation on bioactive-glazed alumina

Cheol Y. Kim*, Sang Soo Jee

Department of Ceramic Engineering, Inha University, 253 Yonghyun-dong, Nam-ku, Incheon, 402-751, South Korea

Received 12 June 2002; accepted 8 November 2002

Abstract

Alumina was coated with bioactive glass which is known to show a bonding behavior to living tissue. Another glass also coated between alumina and bioactive glass to compensate their differences in thermal expansion. After coating the alumina with bioactive glass, it reacted in simulated body fluids to investigate the formation of hydroxyapatite. The bioactive-glazed layer crystallized into α-wollastonite and β-wollastonite crystalline phases when the glaze was fired at 1200 °C and 1100 °C, respectively. When the samples reacted in SBF, α-wollastonite easily leached out of the surface and hydroxyapatite formed on the leached site. The leaching rate of α-wollastonite was faster than that of β-wollastonite, and the hydroxyapatite-forming rate was also faster in the sample containing α-wollastonite than in the other sample. No silica-rich layer was found underneath the newly developed hydroxyapatite.

Keywords: Al_2O_3; Bioactive glass; Hydroxyapatite; Wollastonite

1. Introduction

Hench et al.[1,2] found in the early 1970s that some glasses in the system of Na_2O–CaO–SiO_2–P_2O_5 show a bonding tendency to living tissue in the human body. Since then, various kinds of bioactive glasses and glass-ceramics with different compositions have been introduced.[3–5] However, the applications of most of these materials have been limited to less loaded places in the human body because of their poor mechanical strength.

On the other hand, a high-purity alumina with high-density (>3.9 g/cm^3) was the first bioceramics used for implants.[6] Alumina has been used in load-bearing hip prostheses and dental implants because of its excellent corrosion resistance, high-wear resistance, and strength.[7] This alumina is a bio-inert material and it is safe to use in the human body, but it doesn't bond to living tissue when implanted.

In order to provide bioactivity, one of the bio-inert materials such as titanium metal is often coated with hydroxyapatite.[8,9] Synthetic hydroxyapatite [$Ca_{10}(PO_4)_6(OH)_2$] is very similar to the inorganic components of bone and it has been proven to be bioactive.[10] The most commonly used technique to fabricate hydroxyapatite-coated titanium is by thermal plasma spraying.[11] The chemical composition and structure of the hydroxyapatite coat are often changed during the plasma processing due to high temperature and this affects its bioactivity.[12] The bonding between hydroxyapatite and metal substrate are generally known to be poor.[13]

An alternative method is to coat a bio-inert implant, such as titanium and alumina, with bioactive glass.[14] The coefficient of thermal expansion of bioactive glass is usually much higher than that of bio-inert substrate and this difference may cause cracks in the glass layer.[15] In this study, therefore, another glass layer between bioactive glass and alumina was applied in order to buffer their thermal expansion differences.

The primary objectives of this work are to examine the crystallization of the bioactive glass coat layer depending on the firing temperature and to study the hydroxyapatite-forming behavior depending on the crystalline phases present in the layer coat.

2. Experimental procedure

2.1. Sample preparation

Two different types of glass were prepared as shown in Table 1. One was for a ground-coat glass and the other was for bioactive cover glass, which is now called a

* Corresponding author. Tel.: +82-32-860-7525; fax: +82-32-862-0129.
E-mail address: cheolkim@inha.ac.kr (C.Y. Kim).

0955-2219/03/$ - see front matter © 2003 Elsevier Science Ltd. All rights reserved.
doi:10.1016/S0955-2219(02)00444-2

Table 1
Glass compositions and coefficients of thermal expansion (CTE)

Glass	Composition							
	SiO_2	Na_2O	CaO	B_2O_3	Al_2O_3	P_2O_5	CaF_2	CTE ($\times 10^{-7}$/°C)
Ground coat glass	55	10	25	5	5	–	–	93.4
Bioactive cover glass	55.1	9.2	27.8	–	–	3.4	4.5	108

bioactive glaze. Coefficients of thermal expansion for these glass samples are also included in the table. The coefficient of thermal expansion of alumina used in this study was 88×10^{-7}/°C. Appropriate amounts of raw materials, from the regent grades of SiO_2, $CaCO_3$, Na_2CO_3, H_3PO_4, CaF_2 and Al_2O_3, were weighed and mixed in a gyroblender for 2 h. Then, each glass batch was melted in a Pt-Rh crucible in an electrically heated furnace at the temperature of 1500 °C for bioactive cover glass and 1400 °C for ground-coat glass. The glass melt was cast on a stainless steel plate and was pulverized into the size of less than 10 μm with a planetary agate mill. The glass powder was suspended in an acetone solution and was spray-coated on a disc of dense alumina. The sprayed samples were fired in the tube furnace. The ground coat was fired at 1250 °C for 30 min. and the bioactive glaze coat was fired at 1100 °C or 1200 °C for 30min. The thickness of the coat was 10 μm for the ground coat and 20 μm for the bioactive glaze layer.

For the bulk glass experiment, the glass melt was cast into a graphite mold to make a bar and then the glass bar was annealed at 600 °C before sawing.

2.2. Reaction in simulated body fluids

To examine the hydroxyapatite formation on the bioactive-glazed layer, the bioactive-glazed alumina reacted in simulated body fluids (SBF). SBF was prepared by dissolving NaCl, KCl, $NaHCO_3$, $K_2HPO_4{\cdot}3H_2O$, $MgCl_2{\cdot}6H_2O$, $CaCl_2$ and Na_2SO_4 in tris(hydroxymethyl)-aminomethane[$(CH_2OH)_3CNH_2$] with pH 7.3, as described by Kokubo.[16] The ion concentrations in the solution are almost the same as those of human blood plasma. The prepared samples were suspended in a sealed polyethylene bottle that contained 15.25 ml of SBF. The surface area of the sample to the volume of the solution ratio was 0.1 cm^{-1} and the reaction was carried out at 37 °C at various times.

2.3. Analysis of the reacted bioactive glass coat

The reacted bioactive-glazed layer was examined by a Fourier transform infra-red spectrometer (Bio-Rad FTS 165), thin-film X-ray diffractometer (Philips PW3719 operated at 40 kV, 1.5° at an incident beam angle, Cu target, scan speed: 0.08/s, 2θ: 10–60°) and the scanning electron microscope (Hitachi X-4200, 20 kV).

2.4. Ion concentration measurement in reacted simulated body fluids

The concentrations of Si^{4+} and P^{5+} ions in the reacted SBF were measured by the molybdenum blue method. By adding ammonium paramolybdate solution, the Si^{4+} and P^{5+} ions in the solution turned into silicomolybdate and phosphomolybdate, respectively.[17] The extinctions at 810 nm for silicomolybdate and at 885nm for phosphomolybdate were measured by UV-visible spectrometer (Shimadzu, UV-2401PC) and all extinctions were compared to a standard calibration curve to calculate these ion concentrations.

The concentration of Ca^{2+} ions was examined by an atomic absorption spectrophotometer (Thermo Jarrell Ash Corporation, AA-Scan1).

3. Results and discussion

3.1. Crystallization of bioactive glaze and hydroxyapatite formation

The ground coat was fired at different temperatures ranging from 1100 °C to 1300 °C. We found that the smoothest surface was obtained when the coat was fired at 1250 °C for 30 min. The ground coat contained crystalline phases of anorthite and corundum.[18]

The bioactive glass powder was sprayed on the ground coat and fired at 1100 °C and 1200 °C for 30 min. Each sample reacted with SBF for various times to examine the formation of hydroxyapatite. The obtained hydroxyapatite was examined by a thin-film X-ray diffraction (XRD) and a Fourier Transform Infrared Spectrometer (FT-IR), and their results were shown in Fig. 1 for samples fired at 1100 °C and in Fig. 2 for samples fired at 1200 °C.

When the bioactive-glazed alumina was fired at 1100 °C, the glaze layer crystallized into β-wollastonite with a small amount of fluorapatite (Fig. 1). On the other hand, for the sample fired at 1200 °C, the glaze layer crystallized into α-wollastonite as a major phase with fluorapatite (Fig. 2). This result agreed with the previous study reported by Kim, et al.[19] that stated that the bioactive glass containing a large amount of CaO crystallized into wollastonite when the temperature rose above 1100 °C.

For the sample fired at 1100 °C for 30 min, which contained β-wollastonite crystal, major peaks of β-wol-

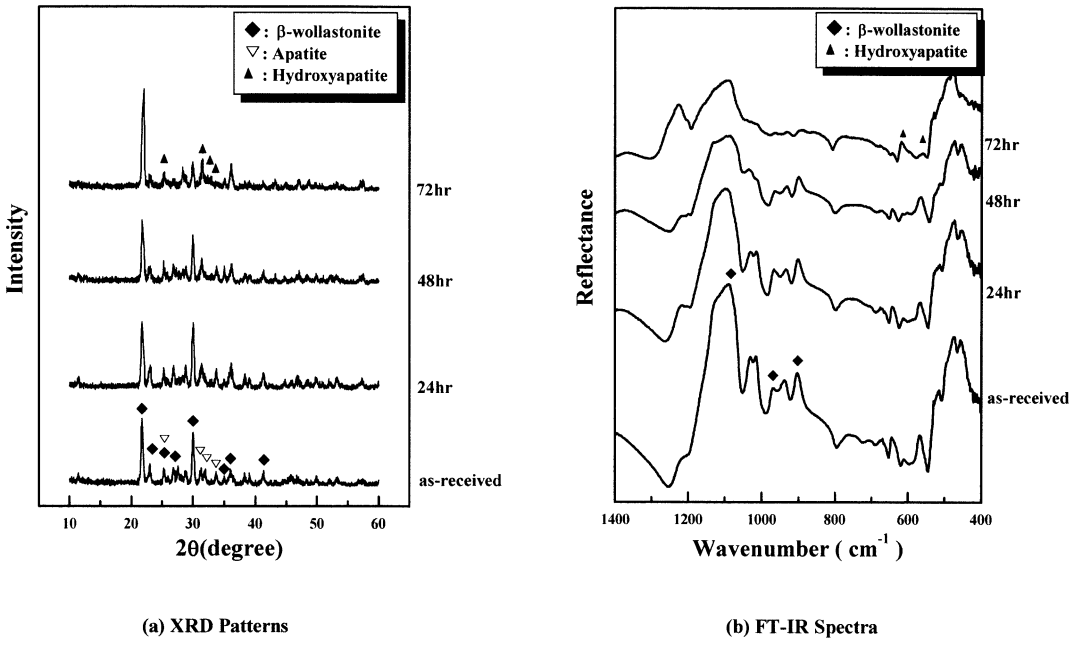

Fig. 1. XRD patterns and FT-IR spectra of bioactive-glazed layer. The layer was heated at 1100 °C for 30 min and reacted in SBF for various times.

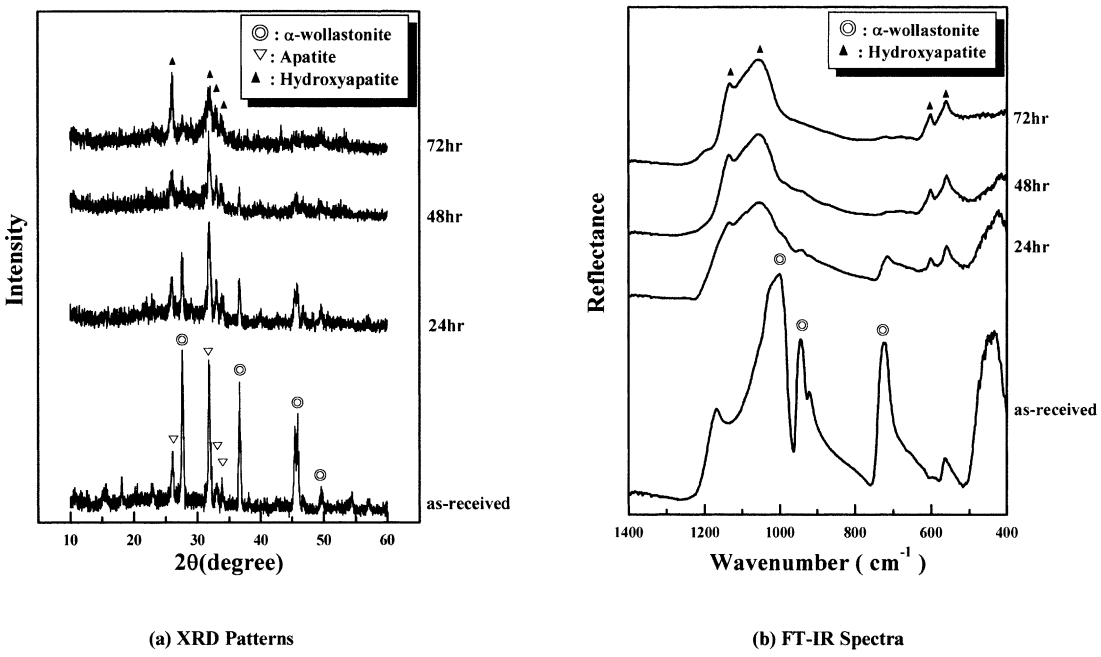

Fig. 2. XRD patterns and FT-IR spectra of bioactive-glazed layer. The layer was heated at 1200 °C for 30 min and reacted in SBF for various times.

lastonite at $2\theta = 20 \sim 25°$ and 30° remained after 72 h of reaction in SBF, and fluorapatite peaks at $2\theta = 30 \sim 35°$ was broadened due to the overlap of hydroxyapatite peaks. However, the peak intensity of hydroxyapatite was relatively smaller than that of β-wollastonite. This result indicates that β-wollastonite could not be leached out easily during reaction in SBF and newly formed hydroxyapatite layer was so thin that XRD could detect β-wollastonite underneath hydroxyapatite layer. FT-IR spectra showed the same results. Because β-wollastonite did not dissolve easily in SBF, main peaks of β-wollastonite[20] at 1090 cm^{-1}, 968 cm^{-1} and 903 cm^{-1} remained after 48 h of reaction, and the intensity of hydroxyapatite peaks at 550 cm^{-1} and 604 cm^{-1} were very low in comparison with the bending vibration peak of Si–O–Si[21] at 475 cm^{-1}. This explains hydroxyapatite did not form well on the surface of bioactive glaze containing β-wollastonite.

For the sample fired at 1200 °C for 30 min, on the other hand, the intensity of α-wollastonite peaks in

XRD decreased rapidly with reaction time, and the characteristic broaden peaks of hydroxyapatite at $2\theta = 30 \sim 35^{\circ}$ appeared after 48 h of reaction. The same result was observed by FT-IR. Most of α- wollastonite peaks[22] at 1000 cm^{-1}, 942 cm^{-1} and 721 cm^{-1} disappeared at 24 h of reaction and the characteristic peaks of hydroxyapatite[23] started to show at 550 cm^{-1} and 604 cm^{-1} at the same reaction time. Those hydroxyapatite peaks grew sharper with reaction time. This indicates that the α- wollastonite crystals in the bioactive coat layer dissolved easily in SBF and thick hydroxyapatite was formed.

These results explain that the hydroxyapatite formation is strongly related to the dissolution rate of α-wollastonite crystals. It is believed that the high leaching rate of Ca^{2+} ions out of α-wollastonite enhances the formation of hydroxyapatite. This explanation is not conclusive at this moment and further studies are needed to verify this.

3.2. Features of hydroxyapatite formation and hydroxyapatite forming rate

Scanning electron microscope (SEM) morphologies of the samples after reaction in SBF for various times were

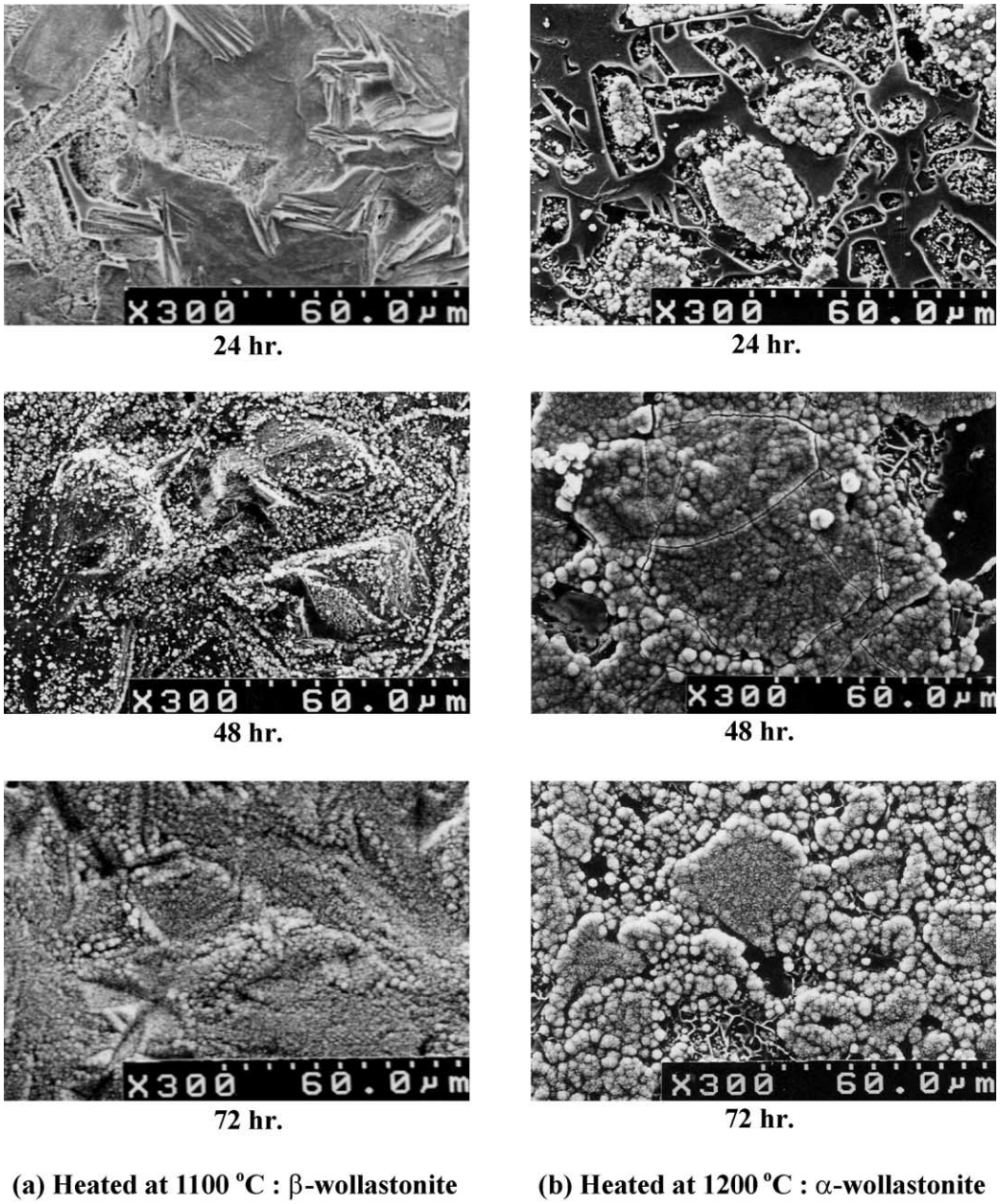

Fig. 3. SEM images of bioactive-glazed layer after reaction in SBF. The layer was heated at 1100 °C and 1200 °C for 30 min and reacted in SBF for various times.

presented in Figs. 3 and 4. Fig. 3 shows the over-all features of hydroxyapatite formation in the long-term exposure to SBF, while Fig. 4 shows the detailed features of hydroxyapatite formation in the early stage of reaction.

When the samples reacted for 24 h, as shown in Fig. 3, a large part of the surface of bioactive-glaze layer fired at 1200 °C was dissolved, while most of the surface of layer fired at 1100 °C remained intact. This is because SBF dissolved α-wollastonite easily, but not β-wollastonite. This agrees well with the previous results shown in Figs. 1 and 2. With an increase in the reaction time, round-shape clusters developed at the site of the dissolved α-wollastonite, but scattered clusters were observed on the sample containing β-wollastonite. Examination of high magnitude SEM revealed that these clusters were the typical leaf-like hydroxyapatite. Moreover, over-all features of samples (Fig. 3) seem that the hydroxyapatite was much denser on the sample containing the α-wollastonite phase. With a further increase in the reaction time, the hydroxyapatite spreads all over the surface for both samples.

Fig. 4 shows the SEM observation of the surface of the bioactive-glazed layer in the early hours of reaction in SBF. For the sample containing β-wollastonite, that was fired at 1100 °C, lots of little seeds of calcium

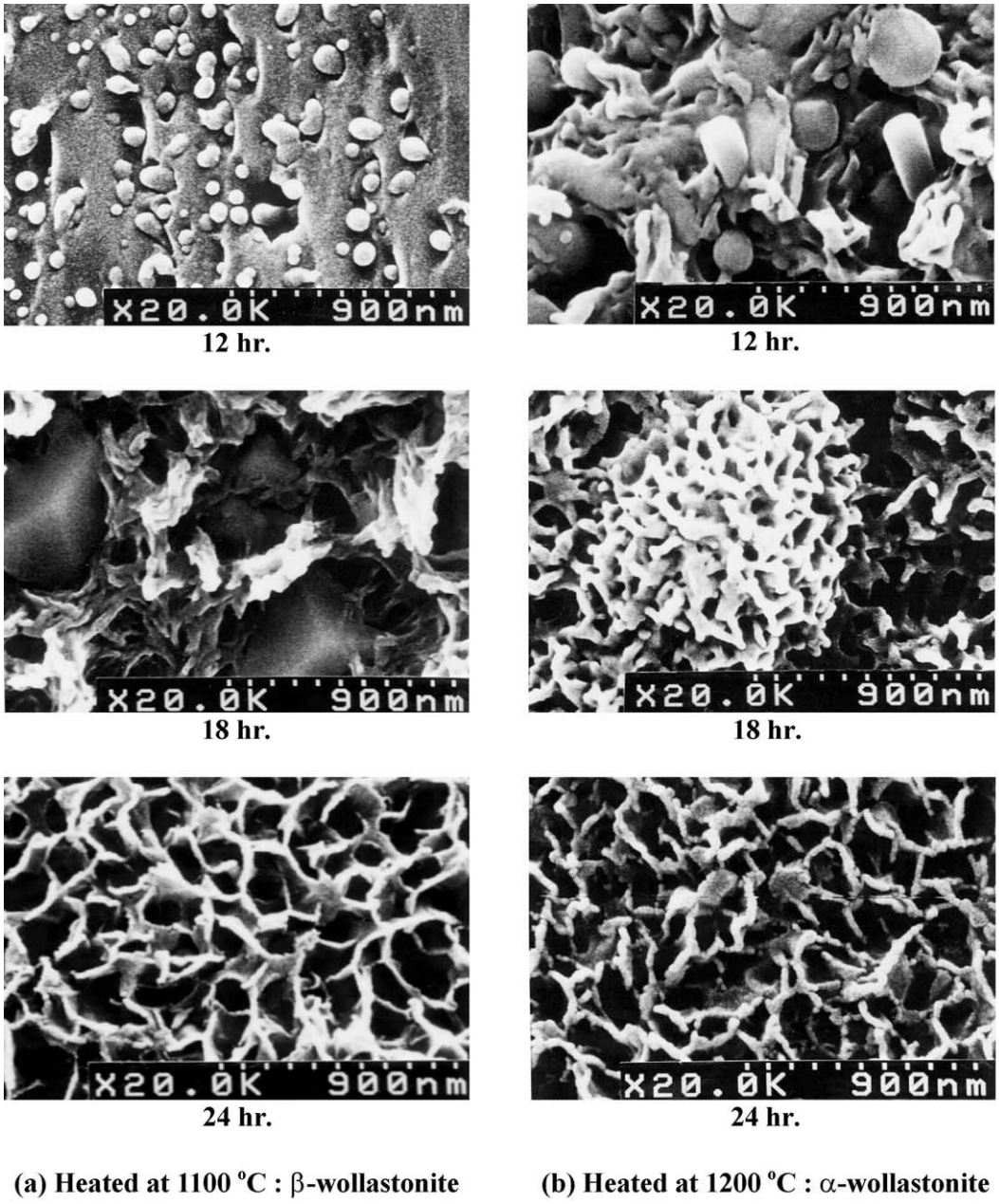

Fig. 4. SEM images of bioactive-glazed layer after reaction in SBF. The layer was heated at 1100 °C and 1200 °C for 30 min and reacted in SBF for various times.

phosphate formed evenly on the entire surface of the sample during 12 h of reaction time and these developed into amorphous calcium phosphate clusters within 18 h of reaction time. Then, these calcium phosphate clusters crystallized into hydroxyapatite crystals after 24 h of reaction. For the sample containing α-wollastonite, that was fired at 1200 °C, amorphous calcium phosphate clusters developed within 12 h of reaction time at the site made by dissolving of α-wollastonite, and then crystallized into hydroxyapatite after 18 h of reaction.

3.3. Ion concentration in SBF

We can also predict the rate of wollastonite leaching and hydroxyapatite formation by measuring the concentrations of ions leached out of samples in the reacted SBF. The concentration of silicon, calcium, and phosphorus ions in the reacted SBF were analyzed with an atomic absorption spectrophotometer and a UV-visible spectrometer, and the results were presented in Fig. 5.

Silicon is a component of wollastonite ($CaSiO_3$) as well as a component of a glass phase, but the SBF does not have this ion. Therefore, the presence of silicon ions in the reacted solution is due to the leaching from the sample. As shown in Fig. 5(a), the leaching rate of the silicon ion was much higher for the sample containing α-wollastonite than for the sample containing β-wollastonite. This explains the higher dissolving behavior of α-wollastonite compared with β-wollastonite as mentioned earlier.

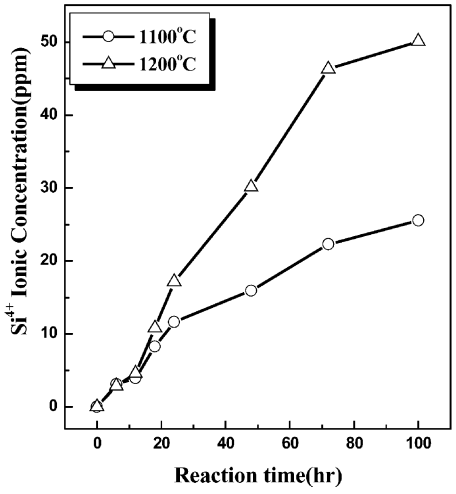

(a) Concentration of Si^{4+} ions

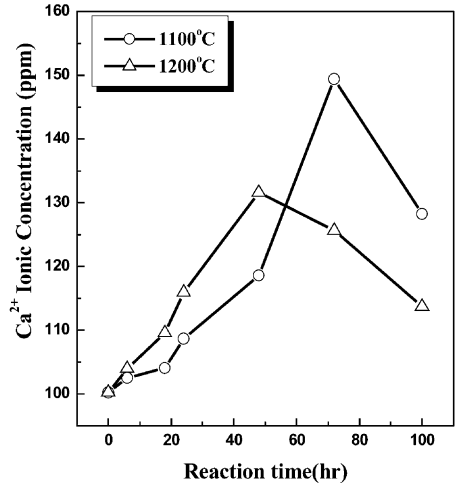

(b) Concentration of Ca^{2+} ions

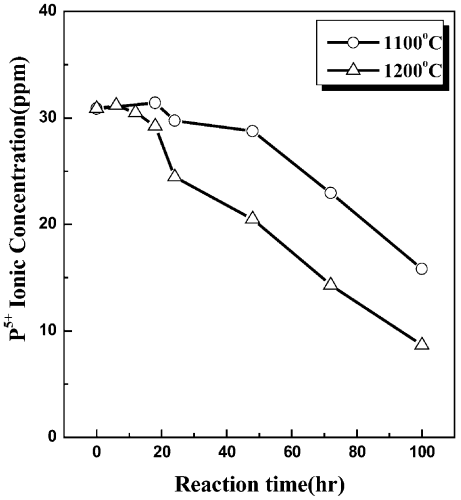

(c) Concentration of P^{5+} ions

Fig. 5. Ion concentrations of SBF after reaction with bioactive-glazed alumina fired at 1100 °C and 1200 °C.

The fresh SBF contained about 100 ppm of calcium ions and its concentration in the reacted solution increased with reaction time in the early stages of reaction, but decreased after a certain period of reaction. As shown in Fig. 5(b), the differences in the ion concentration variation in the two different samples explain that the rate of α-wollastonite leaching was faster than that of β-wollastonite leaching. Moreover, for the sample containing α-wollastonite, the concentration of the calcium ions started to drop after 48 h of reaction time. For the sample containing β-wollastonite, however, the calcium ion concentration increased to 72 h of reaction time. This calcium ion is one of the sources of hydroxyapatite that precipitated onto the sample. The increase in calcium ions was due to the leaching of wollastonite, and the decline of the concentration after specified hours of reaction explains that the up-take rate of the ions that form hydroxyapatite is higher than its leaching rate from the sample. These ion concentration measurements indicate that the hydroxyapatite-forming rate is much faster in the sample containing α-wollastonite than in the sample containing β-wollastonite.

Phosphorus ions are also a component of hydroxyapatite. The original SBF contained about 30 ppm phosphorus ions. As reaction time passed, the concentration of phosphorus ions in SBF decreased because the ions were up-taken on the surface to form hydroxyapatite. The leaching of these ions from the sample is almost negligible because it is believed that most phosphorus ions present in the glass were spent to form the crystallized apatite during the heat-treatment. It is known that fluorapatite is rather chemically stable in SBF.[24] The bioactive glaze contained 3.4 mol % of P_2O_5. The sample containing α-wollastonite consumed more phosphorus ions from SBF than the sample containing β-wollastonite did, indicating that hydroxyapatite forming rate was faster in the α-wollastonite sample than in the β-wollastonite sample.

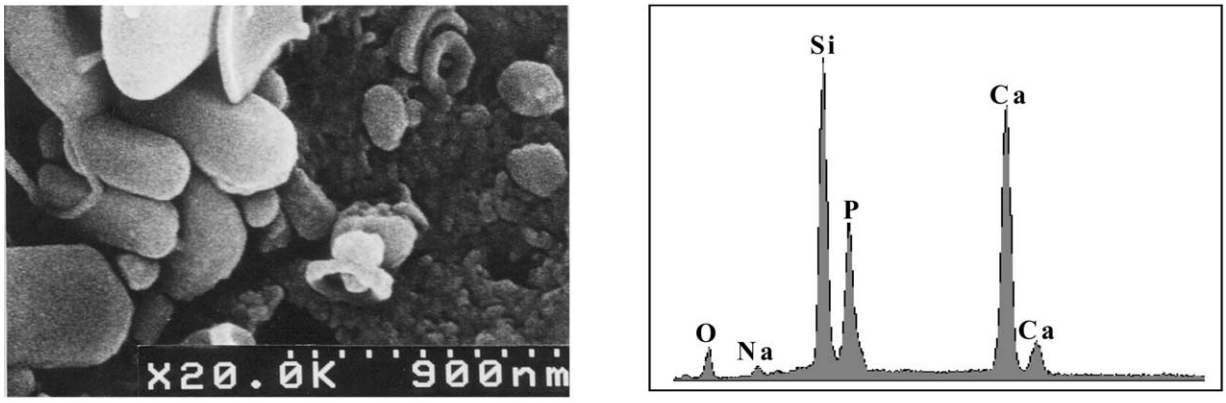

(a) HCl-treated bioactive-glazed layer

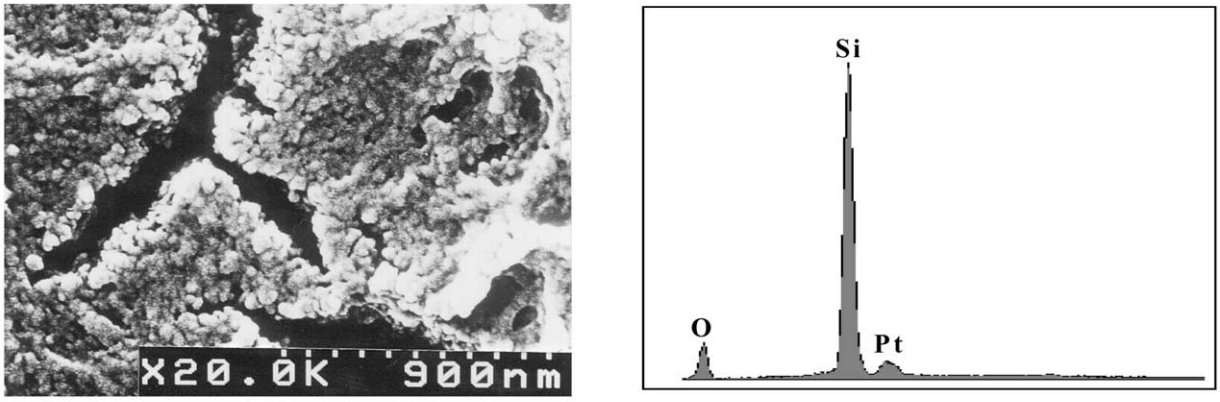

(b) bioactive bulk glass

Fig. 6. SEM images and EDS results of HCl-treated bioactive-glazed layer (a) and bioactive bulk glass (b).

3.4. Hydroxyapatite formation on the HCl-treated coating layer

When bioactive glass reacted in SBF, it has been believed that hydroxyapatite precipitated onto the silica-rich layer that was developed by the leaching of cations from the glass. To examine this phenomenon in this study, two different samples were prepared as follows. First, the sample containing α-wollastonite reacted in SBF for 100 h to obtain hydroxyapatite and then followed by dissolving hydroxyapatite by treating the sample in HCl with pH of 2 for 2 min. Second, the bioactive bulk glass, which has the same composition as the bioactive glaze, reacted in SBF for 100 h.

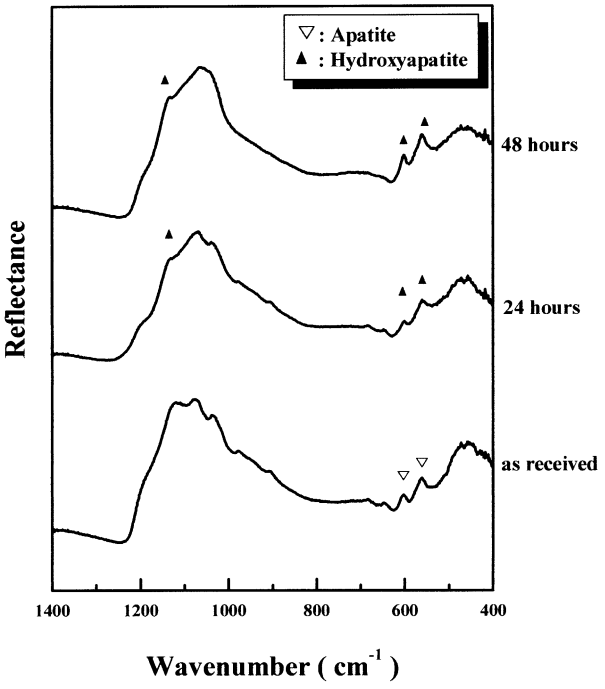

Fig. 7. FT-IR spectra of bioactive-glazed layer after HCl-treatment and the layers after reaction in SBF for various times.

In the bioactive-glazed alumina, as shown in Fig. 6, no silica-rich gel layer underneath the hydroxyapatite was found, instead, some crystalline phases were observed. The XRD study revealed that these crystalline phases were fluorapatite as a major phase and with a small amount of wollastonite.[18] Moreover, an Energy Dispersive Spectroscopy (EDS) result showed Ca^{2+}, Si^{4+} and P^{5+}, which are the elements of wollastonite and glass. This indicates that no silica-rich layer formed in bioactive-glazed alumina. For the bioactive bulk glass, however, no hydroxyapatite was found after 100 h of reaction and a rough surface of a silica-rich layer with some cracks was observed. EDS revealed it was pure silica. Kim and Hench,[25] in the study of Bioglass, argued that an amorphous calcium phosphate film formed on the SiO_2-rich layer first, and then the amorphous film transformed into hydroxyapatite crystalline phase by combining with OH^- and CO_3^{2-} from the solution. This silica-rich layer is a drawback for using bioactive glass for implants because of its weak mechanical strength. In the bioactive-glazed alumina, however, no silica-rich layer was observed as explained above, and this biomaterial could possibly show better performance when it is implanted.

Next, the bioactive-glazed alumina treated with HCl was reacted in SBF again, and its FT-IR results are shown in Fig. 7.

Hydroxyapatite developed again in the bioactive-glazed alumina treated with HCl within 24 h of reaction.

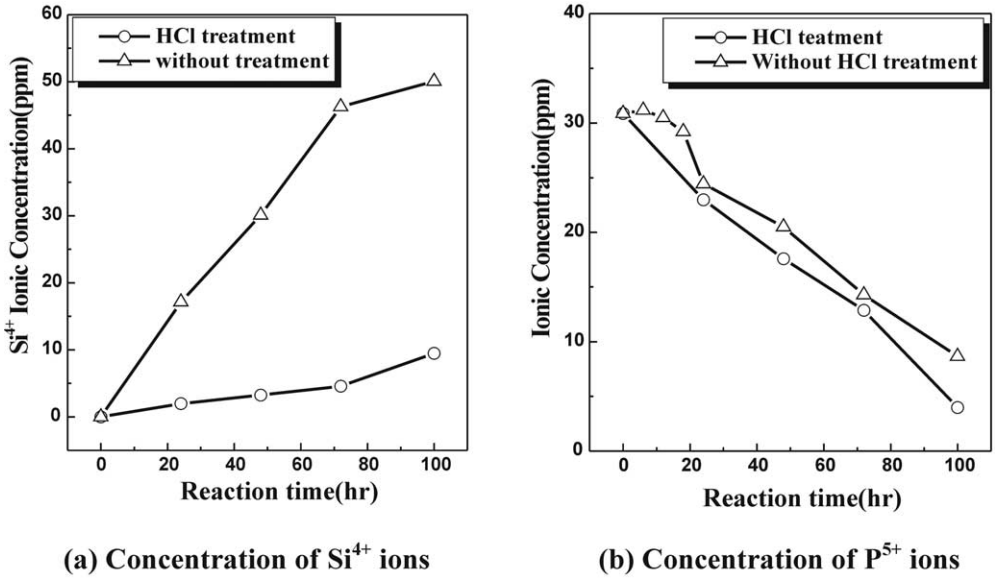

Fig. 8. Comparison of ion concentrations of reacted solution between bioactive-glazed layer after HCl-treatment and untreated sample after reaction in SBF for the various times.

The hydroxyapatite-forming rate of HCl-treated samples was almost the same as that of the non-treated samples (Fig. 2).

We again measured the ion concentrations for the HCl-treated bioactive-glazed alumina after reaction in SBF and the results are shown in Fig. 8. The leaching rate of silicon, which is a component of wollastonite, was much lower in the HCl-treated sample than in the untreated sample. This is because a large amount of wollastonite had already dissolved out. However, the decrease in the concentration of phosphorus ions, which is due to the up-take of the ions from the SBF to form hydroxyapatite, was almost the same for both samples. This explains that even the presence of small amounts of wollastonite in the coating layer after an HCl-treatment will help the formation of hydroxyapatite.

Kokubo[26] argued in his bioactive A/W glass-ceramic studies that the release of considerable amounts of calcium and silicon ions into SBF promotes hydroxyapatite formation. For the present study, however, hydroxyapatite formed easily without a large amount of ion leaching. It is thought that small amount of α-wollastonite which is leached provides a favorable site for hydroxyapatite nucleation like the silica-rich gel layer.

4. Conclusions

When the bioactive-glazed alumina reacted in the SBF, the following conclusions were drawn.

1. When the alumina was coated with bioactive glass and fired at 1100 °C and 1200 °C, the glass coat layer crystallized into β-wollastonite and α-wollastonite, respectively.
2. The rate of α-wollastonite leaching was much faster than that of β-wollastonite leaching when reacted in SBF. Further, the rate of hydroxyapatite formation was faster in the sample containing α-wollastonite than in the sample containing β-wollastonite.
3. The hydroxyapatite-forming rate on the bioactive-glazed alumina was much faster than that for the corresponding bioactive bulk glass.
4. No silica-rich layer was found underneath the newly formed hydroxyapatite in the crystallized bioactive glaze, while the silica-rich layer developed on the corresponding bioactive bulk glass.

References

1. Hench, L. L., Splinter, R. J., Allen, W. C. and Greenlee, T. K., Bonding mechanisms at the interface of ceramic prosthetic materials. *J. Biomed. Mater. Res. Symp.*, 1971, **2**, 117–141.
2. Hench, L. L., Ceramic implants for humans. *Advan. Ceram. Mater.*, 1986, **1**(4), 306–324.
3. Cho, S. B., Miyaji, F., Kokubo, T. and Nakamura, T., Introduction of bioactive glass-ceramic by chemical treatment. *Biomaterials*, 1997, **18**, 1479–1485.
4. Boccaccini, A. R., Machinability and brittleness of glass-caramic. *J. Mater. Process. Technol.*, 1997, **65**, 302–304.
5. Ohtsuki, C., Kushitani, H., Kokubo, T., Kotani, S. and Yamamura, T., Apatite formation on the surface of Ceravital-type glass-ceramic in the body. *J. Biomed. Mater. Res.*, 1991, **25**, 1363–1370.
6. Hench, L. L., Bioceramics:from concept to clinic. *J. Am. Ceram. Soc.*, 1991, **74**(7), 1487–1510.
7. Hench, L. L. and Wilson, J., *An introduction to bioceramics*. World Scientific, Singapore, 1993.
8. Zang, C., Leng, Y. and Zang, X., In vitro stability of plasma-sprayed hydroxyapatite coatings on Ti-6Al-4V implant under cyclic loading. *J. Biomed. Mater. Res.*, 2000, **50**, 267–275.
9. Zeng, H. and Lacefield, W. R., The study of surface tranformation of pulsed laser deposited hydroxyapatite coating. *J. Biomed. Mater. Res.*, 2000, **50**, 239–247.
10. Boretos, J. W., Advances in bioceramics. *Advan. Ceram. Mater.*, 1987, **2**(1), 15–30.
11. Poter, A. E., Hobbs, L. W., Rosen, V. B. and Spector, M., The ultrastructure of the plasma-sprayed hydroxyapatite-bone interface predisposing to bone bonding. *Biomaterials*, 2002, **23**, 725–733.
12. Ha, S. W., Reber, R., Eckert, K. L., Petitmermet, M., Mayer, J. and Wintermantel, E., Chemical and morphological changes of vacuum-plasma-sprayed hydroxyapatite coatings during immersion in simulated physiological solutions. *J. Am. Ceram. Soc.*, 1998, **81**(1), 81–88.
13. Gross, K. A., Gross, V. and Berndt, C. C., Thermal analysis of amorphous phases in hydroxyapatite coatings. *J. Am. Ceram. Soc.*, 1998, **81**(1), 106–112.
14. Hench, L. L., Bioglass Coated Al_2O_3 Ceramics. US Patent 4103002, 1978.
15. Kim, J. K. and Kim, C. Y., Bonding behavior of bioglass coated alumina. *J. Kor. Ceram. Soc.*, 1990, **27**(7), 925–933.
16. Oyane, A., Nakanishi, K., Kim, H. M., Miyaji, F., Kokubo, T., Soga, N. and Nakamura, T., Sol-gel modification of silicon to induce apatite-forming ability. *Biomaterials*, 1999, **20**, 79–84.
17. Parsons T. R., Maita Y., C. Lalli M., *A Manual of Chemical and Biological Methods for Seawater Analysis*. Pergamon Press, 1984, pp. 22–28.
18. Jee S. S., *Behavior of Hydroxyapatite Formation in Bioactive Glass Coated on Alumina*. MS Thesis, Inha University, 2002.
19. Kim, C. Y. and Cho, C. S., Hydroxyapatite formation on bioactive glass-ceramics of $CaO–SiO_2–P_2O_5$ system. *Biomaterial Research*, 1998, **2**(1), 15–20.
20. Cho, S. B., Miyaji, F., Kokubo, T. and Nakamura, T., Induction of bioactivity of a non-bioactive glass ceramic by a chemical treatment. *Biomaterials*, 1997, **18**(22), 1479–7485.
21. Kim, C. Y., Clark, A. E. and Hench, L. L., Compositional dependence of calcium phosphate layer formation in fluoride bioglass. *J. Biomed. Mater. Res.*, 1992, **26**, 1147–1161.
22. Lee E. S., Hydroxyapatite Formation of Crystallized Bioactive Glaze on Alumina. MS Thesis, Inha University, 1995.
23. Filho, O. D., LaTorre, G. P. and Hench, L. L., Effect of crystallization on apatite-layer formation of bioactive glass 45S5. *J. Biomed. Mater. Res.*, 1996, **30**, 509–514.
24. Ahn, H. S., Lee, E. S. and Kim, C. Y., Hydroxyapatite formation on fluoride bioactive glasses coated on alumina. *J. Kor. Ceram. Soc.*, 1999, **36**(10), 1087–1093.
25. Kim, C. Y., Clark, A. E. and Hench, L. L., Early stages of calcium-phosphate layer formation in bioglasses. *J. Non-Cryst. Solid.*, 1989, **113**, 195–202.
26. Kokubo, T., Surface chemistry of bioactive glass-ceramics. *J. Non-Cryst. Solid.*, 1990, **120**, 138–151.